Journal of Petroleum Science and Engineering 211 (2022) 110186

Contents lists available at ScienceDirect

Journal of Petroleum Science and Engineering

journal homepage: www.elsevier.com/locate/petrol

Oil sources and accumulation processes of the Neoproterozoic Luotuoling Formation reservoirs (~930 Ma) in North China Craton

Hong Xiao [a,b], Tieguan Wang [a,b], Meijun Li [a,b,c,*], Dongxia Chen [a,b], Jian Chang [a,b], Daofu Song [a,b], Chengyu Yang [a,b], Yingjie Hu [d], Sajjad Ali [a,b]

[a] State Key Laboratory of Petroleum Resources and Prospecting, China University of Petroleum, Beijing, 102249, China
[b] College of Geosciences, China University of Petroleum, Beijing, 102249, China
[c] Key Laboratory of Exploration Technologies for Oil and Gas Resources, Ministry of Education, College of Resources and Environment, Yangtze University, Wuhan, Hubei, 430100, China
[d] Research Institute of Petroleum Exploration and Development, Liaohe Oilfield Company, PetroChina, Panjin, Liaoning, 124010, China

ARTICLE INFO

Keywords:
Oil sources
Oil-source correlation
Proterozoic
Liaoxi depression
North China Craton

ABSTRACT

Oil sources and accumulation processes of the Neoproterozoic Luotuoling Formation (~930 Ma) in the Liaoxi Depression are investigated using integrated fluid inclusion, basin modelling and oil-source rock correlation analyses. In the upper Luotuoling Formation sandstone reservoir in Han-1 well, abundant bitumen inclusions and white fluorescent bitumen-bearing oil inclusions were observed. Combined with microthermometry of aqueous inclusions and burial history analysis, the oil charge time of the upper Luotuoling Formation sandstone reservoir took place at approximately 465–455 Ma. This oil was derived from the Gaoyuzhuang Formation source rock according to biomarkers and isotope compositions. However, oil generation of the Gaoyuzhuang Formation had already ended before 455 Ma, so the oils cannot be generated directly from the Gaoyuzhuang Formation source rocks, but definitely migrated from the destroyed paleo-oil accumulations in the Wumishan or Tieling formations. In addition, the lower Luotuoling Formation sandstone reservoir contains mainly yellowish orange fluorescent oil inclusions. The oil in the lower Luotuoling Formation sandstone reservoir was directly generated from the Hongshuizhuang source rock at 240–230 Ma. The study on oil accumulation history of the Neoproterozoic Luotuoling Formation reservoir is significant for further exploration of Proterozoic petroleum resources in the Liaoxi Depression, North China Craton.

1. Introduction

Precambrian petroleum has been considered as a unique and potentially large resource. However, in the early stages of Precambrian oil exploration, most researchers were skeptical of Precambrian petroleum potential. Many petroleum explorationists supposed that the distribution of commercial hydrocarbon accumulations generated from Precambrian source rocks was unusual because of the extended period of opportunities for the rocks to be destroyed through thermal degradation and/or other geological processes (Fowler and Douglas, 1987). Since the 1970s, however, numerous oil and gas reservoirs in Meso-Neoproterozoic rocks have been recognized worldwide, particularly in China (Wang, 1980; Hao and Feng, 1982; Wang and Simoneit, 1988; Liu and Fang, 1989), Siberia (Murray et al., 1980; Kuznetsov, 1997), India (Peters et al., 1995; Dutta et al., 2013), Oman (Grantham et al., 1987, 1990; Terken and Frewin, 2000) and Australia (Jackson et al., 1986; Volk et al., 2005). The oldest live oil discovered was generated from the Velkerri Formation (~1420–1360 Ma) within the Roper Group in the McArthur Basin (Jackson et al., 1986; Crick et al., 1988), which belongs to the same age as the oil seepages within the Mesoproterozoic reservoirs (~1450–1320 Ma) in the North China Craton (NCC). Over past decades, interest in the Precambrian oil and gas system has grown, and they have become regarded as potentially, largely and relatively unexplored frontier opportunities in the petroleum industry (Craig et al., 2009).

In China, Meso-Neoproterozoic strata are well developed through of the Yanliao Faulted-Depression Zone (YFDZ), which is situated in northernmost NCC (Fig. 1). By the end of 2009, 223 sites of oil seepages have been found in the YFDZ, and 86 of them exist in the Liaoxi Depression, which are widely distributed in the Mesoproterozoic-

* Corresponding author. State Key Laboratory of Petroleum Resources and Prospecting, China University of Petroleum, Beijing, 102249, China.
E-mail address: meijunli2008@hotmail.com (M. Li).

https://doi.org/10.1016/j.petrol.2022.110186
Received 7 May 2021; Received in revised form 28 December 2021; Accepted 17 January 2022
Available online 20 January 2022

Neoproterozoic reservoirs of the Wumishan, Tieling and Luotuoling formations (Wang et al., 2016). Since 1978, eleven wells have been drilled into the Meso-Neoproterozoic formations in the Jibei and Liaoxi depressions, namely JQ-1, JQ-3, Shuang-1, Kuan-1, Jiyuan-1, Yang-1, Han-1, Xinglong-1, LLD-1, LLD-2 and ND-1 wells. Although most wells have obvious oil shows, no significant commercial oil and gas accumulation has been discovered in the Meso-Neoproterozoic sequences. The lack of seismic data and insufficient research on hydrocarbon accumulations have led to the failed exploration of the Proterozoic petroleum resources systems (Sun and Wang, 2016).

Previous studies mostly focused on the Jibei and Xuanlong depressions, and largely addressed the analyses of biomarker compositions in Proterozoic rock (Wang and Simoneit, 1995; Peng et al., 1998; Li et al., 2001, 2003), paleo-environment (Luo et al., 2015; Tang et al., 2016, 2017), biological source and evolution (Zhu and Chen, 1995; Peng et al., 2009; Guo et al., 2013; Luo et al., 2016; Zhu et al., 2016; Qu et al., 2018) and oil-source correlation (Wang et al., 2016). However, few studies have addressed the oil generation and charge histories of the Liaoxi Depression (Dai et al., 2014), which has restricted the process of Meso-Neoproterozoic petroleum exploration in this region. In this study, the Mesoproterozoic Gaoyuzhuang black argillaceous dolomite Formation (JQ-3 well) and Hongshuizhuang black shale (JQ-1 well), and the Neoproterozoic Luotuoling sandstone core samples (Han-1 well) were collected and geochemically analyzed. The main objectives of this study are the determination of the oil generation histories of the Meso-proterozoic source rocks, oil sources and oil accumulation processes of the Neoproterozoic Luotuoling Formation oil reservoir.

2. Geological setting

The YFDZ with an area of roughly 10.6×10^4 km^2 is situated in the Yanshan area of the NCC (Sun and Wang, 2016). The Meso-Neoproterozoic sequences are widely and well preserved in the YFDZ, which is the oldest oil-bearing structural unit in China (Wang et al., 2019, 2020). The YFDZ starts from Zhangjiakou City in the west and reaches Fuxin City in the east, and can be further divided into five depressions and two uplifts: Xuanlong Depression, Jingxi Depression, Jidong Depression, Jibei Depression, Liaoxi Depression, Shanhaiguan Uplift and Mihuai Uplift (Fig. 1) (Wang et al., 2016).

Two large-scale contractional tectonic events occurred during the Proterozoic, resulting in two major unconformities in the YFDZ (Meng et al., 2011). The first crustal contraction occurred between 2.0 and 1.8 Ga corresponding to the formation of the Supercontinent Columbia, which is usually called the Lvliang Movement in the NCC (Lu et al., 2002; Zhao et al., 2002). The second crustal contraction formed a regional unconformity between the Mesoproterozoic Xiamaling Formation and Neoproterozoic Luotuoling Formation in response formation of Rodinia around 1.0 Ga, which is known as the Yuxian Movement in the NCC (Fig. 2) (Meng et al., 2011).

The YFDZ received a set of extremely thick and stable marine carbonate-clastic rock sequences above the Archean metamorphic basement, with a total thickness of more than 8000–9000 m during the Meso-Neoproterozoic. This set of unmetamorphosed sedimentary rocks are well-exposed and widely distributed in the NCC, which is composed of the Paleoproterozoic Changcheng (Statherian), the Mesoproterozoic Jixian (Calymmian), the Mesoproterozoic Unnamed-1 (Ectasian), the Mesoproterozoic Unnamed-2 (Stenian) and the Neoproterozoic Qingbaikou systems (Tonian) in ascending order, and without the Nanhuan (780–635 Ma) and Sinian (635–542 Ma) systems (Fig. 2) (Qiao et al., 2007; Li et al., 2009; Gao et al., 2011). Moreover, Niu and Xin (2013) newly established the Jinzhou System (1400–1200 Ma) instead of the Unnamed-1 system (Ectasian) (Niu and Xin, 2013), which may be increasingly accepted. According to the latest studies on the Precambrian stratigraphic column of the NCC (Gao et al., 2010, 2011; Niu and Xin, 2013), the Gaoyuzhuang Formation (Jx*g*) was reclassified from the Changcheng System to the Jixian System, and the Jinzhou System (Pt_2^3, 1400–1200 Ma) only comprises the Xiamaling Formation (Jz*x*) (Fig. 2).

The black shale of the Mesoproterozoic Hongshuizhuang Formation was regarded as the most effective source rock in the study area (Hao and Feng, 1982; Liu and Fang, 1989). In addition, several studies have revealed that the total thickness of the Mesoproterozoic Gaoyuzhuang black argillaceous dolomites in the Jibei Depression with high organic matter abundance (TOC >0.5%) is up to 164 m, and the average TOC value is 1.16% with the maximum up to 4.29% (Wang et al., 2016), which represents moderate to good source rock. Moreover, the early oil filling of the Mesoproterozoic Xiamaling Formation bituminous sandstone reservoir in the Jibei Depression was considered to be sourced from the Gaoyuzhuang Formation (Wang and Han, 2011). The oil sources analysis based on molecular markers showed that almost all the oil-seepages found in the Wumishan and Tieling formations and the late oil filling of Xiamaling Formation bituminous sandstone reservoir were sourced from the Hongshuizhuang Formation (Wang et al., 2016).

A comprehensive analysis of the fossil assemblage of macroscopic algae (*Chuaria-Tawuia-Longfengshania*) and SHRIMP zircon U–Pb ages determined a weighted mean $^{206}Pb/^{238}U$ age of 930 ± 10 Ma for the

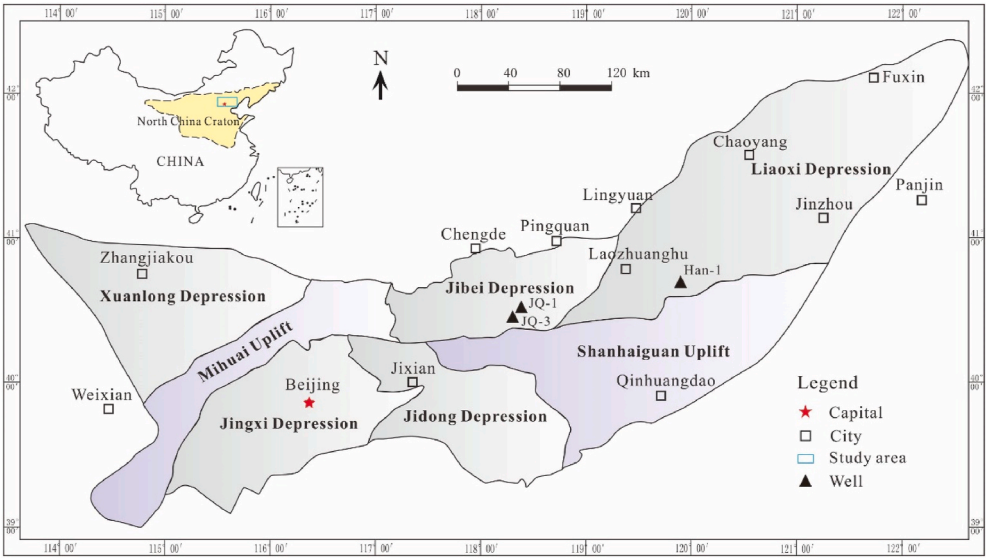

Fig. 1. Map of geographic location and tectonic units of the Yanliao Faulted-Depression Zone, North China Craton (modified after (Wang et al., 2016).

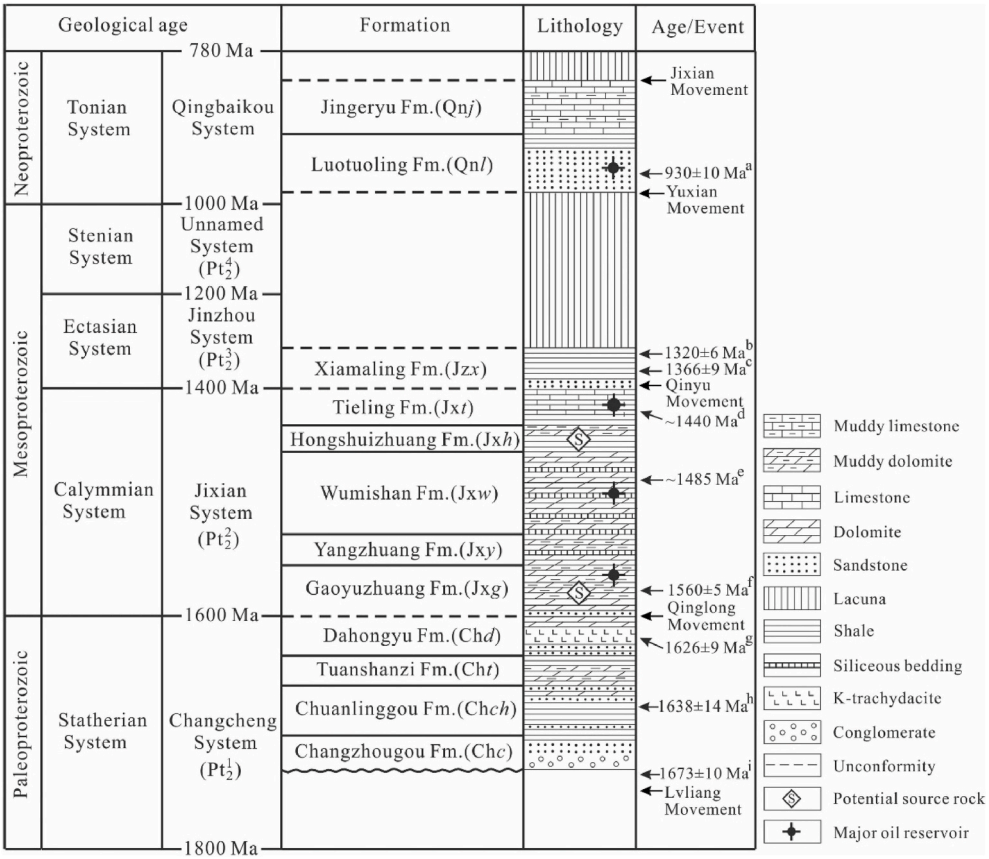

Fig. 2. Stratigraphic column of the Meso- and Neoproterozoic section of the Yanliao Faulted-Depression Zone, North China Craton (modified after (Meng et al., 2011; Wang et al., 2016)). a=(Gao et al., 2009; Niu and Xin, 2013); b=(Li et al., 2009); c=(Gao et al., 2008a); d=(Li et al., 2010, 2014; Su et al., 2010); e=(Li et al., 2014); f=(Li et al., 2010a); g=(Gao et al., 2008b); h=(Gao et al., 2009); i=(Li et al., 2011).

Luotuoling Formation, which belongs to the Neoproterozoic Qingbaikou System (Gao et al., 2009; Niu and Xin, 2013). The drilling depth of Han-1 well (Fig. 1) in the Liaoxi Depression is 2667.0 m, which consists of the Cretaceous Yixian Formation, Cambrian Zhangxia, Xuzhuang, Mantou and Changping formations, Neoproterozoic Luotuoling Formation, and Mesoproterozoic Tieling, Hongshuizhuang and Wumishan formations, from top to bottom. However, because the thickness of the Wumishan Formation generally exceeds 3000 m in the study area, which has not been penetrated completely in the Han-1 well. Interestingly, the Han-1 well drilled the full section of the Luotuoling Formation with a thickness of 81 m (2090.0–2171.0 m), which is generally composed of the lower sandstone interval and upper purple shale interval. The sandstone reservoir within the depth of 2145.0–2163.0 m has excellent oil shows, indicating that the Neoproterozoic Luotuoling Formation in the Liaoxi Depression is a set of potential reservoir rocks worthy of notice.

3. Samples and methods

3.1. Samples

LX2 and LX3 sandstone samples were taken from the Dahongyu and Changzhougou formations of the Mesoproterozoic Changcheng system, respectively, which were taken from the outcrop of the Laozhuanghu area in the Liaoxi Depression (Fig. 1). Zircon grains were separated using conventional heavy-mineral separation techniques from these sandstones.

Six sandstone core samples from the Neoproterozoic Luotuoling Formation with the depths in the range of 2125.12–2154.04 m were collected from the Han-1 well. Logging and core data showed a good oil shows in this sandstone member, and petrographic and microthermometric analysis were performed in the study. In addition, the Mesoproterozoic Gaoyuzhuang and Hongshuizhuang formations source rocks were collected from the JQ-1 and JQ-3 wells in the YFDZ, NCC (Fig. 1). Nine samples of the Cretaceous, Cambrian and Proterozoic from the Han-1 well were collected for the bitumen reflectance (R_B).

3.2. Methods

3.2.1. Fluid inclusion microthermometry

Petroleum fluid inclusions, which record oil charge events, provide the direct and reliable information for the nature of oil-bearing fluids at different times in the geological past (McLimans, 1987; Volk and George, 2019). Also, inclusions can be well-preserved during a long geological history without either being destroyed by tectonic events or later contaminated, and thus the hydrocarbons trapped in the inclusions can provide new insights that are unobtained from present-day fluids alone (Volk and George, 2019).

Fluid inclusions and petrography characteristic of sandstone core samples from the Neoproterozoic Luotuoling Formation were observed by a Leica transmitted microscope equipped with a polarizer and incident light lamp. A Linkam THMSG600 heating-freezing stage was used to perform microthermometric measurement at China University of Petroleum, Beijing (Ni et al., 2016; Yang et al., 2018). The homogenization temperatures (T_h) were obtained using a heating program. The heating rate of each heating during the initial stage is 10 °C/min, which is adjusted to 1 °C/min when inclusion is close to the phase charge points. The final ice melting temperature ($T_{m,\ ice}$) was measured using a heating/cooling rate of 1 °C/min. The T_h and $T_{m,\ ice}$ for fluid inclusions were acquired by cycling measurement (Goldstein and Reynolds, 1994),

and the measurement of T_h were performed before that of $T_{m,\ ice}$ to avoid the impacts on T_h when freezing the fluid inclusion. Salinities of aqueous-fluid inclusions were calculated using ice points of H_2O–NaCl (Bodnar, 1993). Moreover, fluid inclusions that show necking down, leakage, stretching or whose relationships with their host minerals ruled out (Goldstein, 2001).

3.2.2. Biomarker analysis

In order to improve the accuracy and reliability of experimental results of this study, all analyzed rock samples are drilling cores rather than cuttings or field outcrops. The pretreatment of rock samples, soluble organic matter extraction, group components separation, and gas chromatography and mass spectrometry (GC-MS) were conducted at China University of Petroleum, Beijing. All core samples (e.g. source rocks and oil sands) were initially cleared with distilled water and then dried in oven. After that, the exterior portion was removed before crushing the sample, and the interior portions were further soaked and washed with dichloromethane (CH_2Cl_2) (Xiao et al., 2021a, 2021b). More than 150 g of powdered interior portions was extracted for 72 h using Soxhlet apparatus. The asphaltenes in the extracts were precipitated using *n*-hexane and filtered with filter papers after 24 h, and then the residual solution was fractionated into three components: saturated hydrocarbon; aromatic hydrocarbon; and resin fraction by liquid chromatography. The GC-MS analysis of saturated molecular markers used an Agilent 6890 gas chromatograph and an Agilent Model 5975i mass selective detector. More detailed temperature program and conditions refer to Xiao et al. (2019a).

3.2.3. Thermochronology

Zircon (U–Th)/He (ZHe) dating was conducted at the Institute of Geology and Geophysics, Chinese Academy of Sciences (IGGCAS), and the detailed method was described by (Wu et al., 2018). A brief description of this experimental procedure is as follows: (1) selected 3 zircon grains without inclusion and fractures; (2) the measurement of Helium (He) were performed using a fully automatic He extraction system; (3) After He measurement, zircon grains were transferred to 350 μL Savillex PFA vials (Evans et al., 2005), and added standard solution; (4) Using Thermal Fisher X-Series II inductively coupled plasma mass spectrometry to determine the U and Th concentration of zircon grains; (5) Using Helioplot program to calculate (U–Th)/He age (Vermeesch, 2010). Finally, the ages were corrected for α emission (Gautheron et al., 2009).

4. Results and discussion

4.1. Fluid inclusion

4.1.1. Petrography characteristic

Lithologically, the Luotuoling Formation mainly contains quartz sandstone, forming a potential reservoir with a purple shale as seal (Fig. 3). According to the physical property data of the Luotuoling Formation sandstone provided by the Liaohe Oilfield Company, the porosity of the upper Luotuoling Formation sandstone (2153.01–2154.04 m) is 6.6%, while the lower Luotuoling Formation sandstone (2153.01–2154.04 m) is only 3.0%, indicating the upper sandstone has better reservoir physical properties than that of lower sandstone.

Moreover, optical characteristics of hydrocarbons in intergranular pores are markedly different between the upper and lower Luotuoling Formation sandstones. The intergranular pores of the upper sandstone are filled with solid bitumen which is opaque in transmitted light (Fig. 3a) and non-fluorescent under UV light (Fig. 3b). The presence of bitumen is interpreted to represent paleo-oil accumulation having undergone thermal degradation, biodegradation, or/and oxidation. In contrast, the pores of the lower sandstone contain free oil with yellowish orange fluorescence under UV light (Fig. 3c and d).

4.1.2. Fluorescence color and Raman spectrum analyses

Oil-bearing inclusions record the features of oils that charged the reservoir at different geological times. Hydrocarbons within oil-bearing inclusions with different physico-chemical attributes usually show various fluorescence colors (Stasiuk and Snowdon, 1997), which can be used to qualitatively evaluate thermal maturity. It has been proposed that the blue region of the visible spectrum usually indicates inclusion

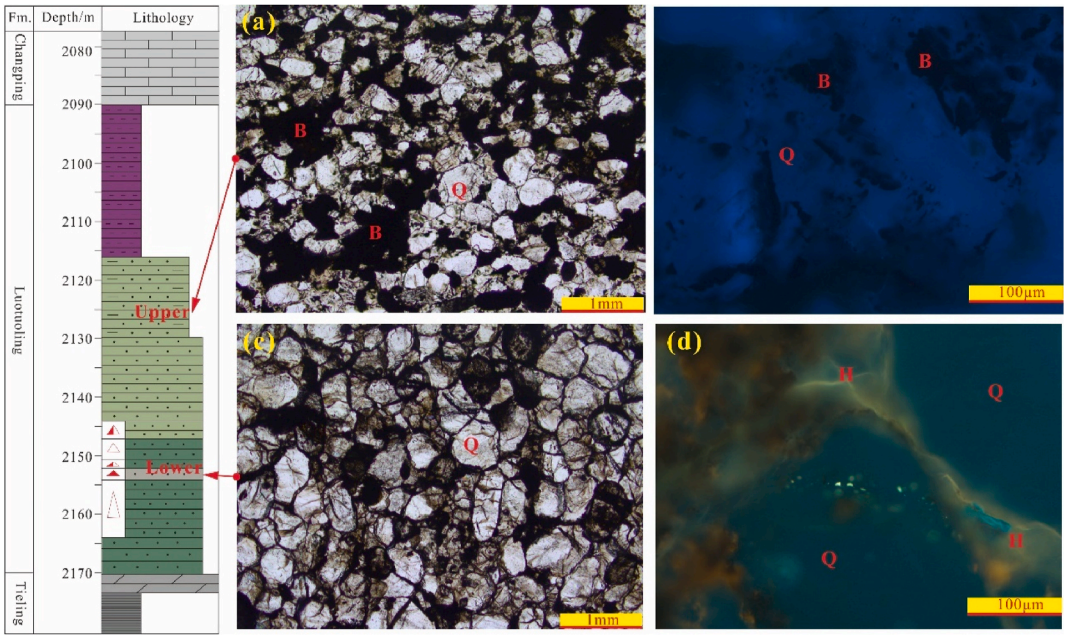

Fig. 3. Characteristics of Neoproterozoic Luotuoling Formation sandstones in the Han-1 well under transmitted light and UV light. (a–b) showing the intergranular pores are filled with solid bitumen in the sample at 2125.12–2128.88 m; (c–d) showing the intergranular pores filled with yellowish orange fluorescence free oil in the sample at 2153.01–2154.04 m (B = solid bitumen; Q = quartz; H = hydrocarbon/oil; φ = porosity). (For interpretation of the references to color in this figure legend, the reader is referred to the Web version of this article.)

oils with high maturity, whereas the red region represents a relative low maturity (Burruss et al., 1985; Goldstein and Reynolds, 1994).

Different types of the hydrocarbon fluid inclusions in the Luotuoling Formation sandstone reservoirs in the Han-1 well were observed. In the upper Luotuoling Formation reservoir (2125.12–2128.88 m), the bitumen inclusions (Fig. 4a and b) and bitumen-bearing oil inclusions (Fig. 4c and d) were abundant and widely distributed along healed micro-fractures. The oil of bitumen-bearing oil inclusions mainly shows white fluorescence (Fig. 4d). Based on Raman spectra analysis of the bitumen-bearing oil inclusions, the black part along the inner edges of the inclusions are proved to be bitumen (Fig. 5). The Raman spectrum of the bitumen is characterized by the peaks of 1343.36 cm^{-1}, 1604.80 cm^{-1}, 2924.03 cm^{-1} and 3190.77 cm^{-1}, which are the diagnostic peaks of solid bitumen (Zhang et al., 2009). The white fluorescence of oil and the presence of bitumen in inclusions are probably representative of a high degree of thermal evolution (George et al., 2001; Yang et al., 2018). In contrast, the oil inclusions in the lower Luotuoling Formation reservoir (2153.01–2154.04 m) have yellow fluorescence, which is generally distributed in transgranular micro-fractures in detrital quartz grains (Fig. 4f and h). Overall, it can be proposed that the upper and lower sandstones reservoirs have experienced different oil charge and accumulation histories.

4.2. Oil-source rock correlation

In order to clarify the differential distributions of bitumen and oil inclusions in the upper and lower Luotuoling Formation reservoirs, oil to source rock analysis was further conducted.

4.2.1. Distribution of rearranged hopanes

C_{30} hopane and C_{31}–C_{35} homohopanes are widely accepted to be derived from prokaryotic microorganisms (Ourisson et al., 1987). Moreover, the formation conditions and biological source of rearranged hopanes has been controversial (Philp and Gilbert, 1986; Killops and Howell, 1991; Moldowan et al., 1991; Farrimond and Telnæs, 1996; Xiao et al., 2021a), but several recent studies have extended their application in oil family classifications and oil-source correlation (Zhu et al., 2007; Xiao et al., 2019a, 2019b). The different type of rearranged hopanes present obvious variations of their relative abundance in our samples (Fig. 6). Interestingly, the 17α(H)-diahopanes (e.g., C_{29}Dia and C_{30}Dia) and 18α(H)-neohopanes (Ts and C_{29}Ts) are identified and abundantly distributed in the oil sands of the lower Luotuoling Formation sandstone reservoir with the depth of 2153.01–2154.04 m (Fig. 6c) and in the Hongshuizhuang Formation source rock extracts (Fig. 6d), but very low abundance in the oil sands of the upper Luotuoling Formation sandstone reservoir with the depth of 2125.12–2128.88 m (Fig. 6a) and the Gaoyuzhuang Formation source rock extracts (Fig. 6b). Xiao et al. (2021a) proposed that the variable abundance of rearranged hopanes in the Mesoproterozoic sediments of NCC is predominantly effected by biological source and sedimentary environment. Another possible reason for the completely different distribution of rearranged hopanes is that the amount of clay minerals contained in the Hongshuizhuang Formation black shale is much higher than in the Gaoyuzhuang Formation black micritic dolomite. In a word, the rearranged hopanes distribution can be effectively used as a diagnostic biomarker to distinguish whether the oils were generated from the Gaoyuzhuang Formation or the Hongshuizhuang Formation source rocks.

4.2.2. Distribution of 13α(alkyl)-tricyclic terpane series

Wang (1989) first detected and identified a new series of biomarker compounds, namely C_{18}–C_{23} 13α(alkyl)-tricyclic terpanes, in the basal bituminous sandstone fossil-oil-reservoirs within the Mesoproterozoic Xiamaling Formation in the Lingyuan County, Liaoning Province (Wang, 1989; Wang and Simoneit, 1995). Up to now, the new series of 13α (alkyl)-tricyclic terpanes has only been reported in the Meso- and Neoproterozoic source rocks and related oils (Luo et al., 2016; Xiao et al., 2021b), and has not been detected in Phanerozoic rocks and related oils. Thus, it can be speculated that it is a diagnostic biomarker series for Proterozoic organic matter (Xiao et al., 2021b). Furthermore, catalytic hydropyrolysis experiments were carried out on the kerogen of three sets of potential source rocks (Gaoyuzhuang Formation black micritic dolomite, Hongshuizhuang and Xiamaling formations black shales) to analyze and compare their biomarker compositions. The results of experimental analysis showed that the C_{18}–C_{23} 13α(alkyl)-tricyclic terpanes were absent in the kerogen of the Gaoyuzhuang Formation, but completely distributed in the kerogen of the Hongshuizhuang Formation as a unique biomarker (Wang et al., 2016).

In the study, a distinct and complete distribution of the C_{18}–C_{23} 13α (alkyl)-tricyclic terpanes were also identified in the oils in the lower Luotuoling Formation sandstone reservoir (Fig. 7c) and the Hongshuizhuang Formation source rocks (Fig. 7d), which is coincident with the previous research by Wang et al. (2016). The oils in the upper Luotuoling Formation sandstone reservoir and the Gaoyuzhuang Formation source rock extracts show a similar feature, without C_{18}–C_{23} 13α (alkyl)-tricyclic terpane series (Fig. 7a and b).

4.3. Oil generation modelling

Interestingly, the upper and lower Luotuoling Formation sandstone oil reservoirs present obviously different oil sources. Therefore, the accumulation process of the Luotuoling Formation reservoirs were further analyzed. Basin modelling is increasingly becoming an essential tool in oil and gas exploration (Waples, 1994), which can simulate the generation, secondary migration and accumulation processes of hydrocarbons in a petroliferous basin (Magoon and Dow, 1994).

4.3.1. Burial history

In this study, burial history and thermal maturity diagrams were created using BasinMod 1D software. Parameters, such as lithology, thickness, erosion, deposition, hiatus and present depth were obtained for the Han-1 well using unpublished data from the Liaohe Oilfield Company and published papers (Dai et al., 2014; Sun and Wang, 2016). The Proterozoic stratigraphic ages are based on the latest Precambrian stratigraphic column of the NCC discussed by the Subcommission on Precambrian of National Commission on Stratigraphy of China in 2009 and 2010 (Gao et al., 2011). The basin experienced multiple stages of tectonic movement, including the Himalayan, Yanshan, Indosinian, Caledonian, Yuxian and Qinyu movements, resulting in a loss of strata (e.g. Mesoproterozoic Unnamed System, Silurian, Devonian and Jurassic System) in the study area. The thicknesses of the Gaoyuzhuang, Yangzhuang and Wumishan formations in the study were calculated by a time-to-depth conversion based on a seismic-reflection profile (95091015-JC), because the Han-1 well was not drilled through the Mesoproterozoic Wumishan Formation.

All strata are composed of mixed lithology, therefore their physical properties (e.g. density, initial porosity, and thermal conductivity) were calculated by the relevant properties of each pure lithology in percentage. For example, thermal conductivity matrix values of 1.5 W/(m·K) for shale, 4.4 W/(m·K) for sandstone and 4.8 W/(m·K) for dolomite in the BasinMod system were used in modelling the temperature field. Based on these data, the burial history of Han 1 well was reconstructed (Fig. 8).

4.3.2. Thermal history inversion

The ZHe ages of zircon grains from the Dahongyu Formation (LX2 samples) and Changzhougou Formation (LX3 samples) are in the range of 141.4–155.0 Ma and 130.1–145.5 Ma, respectively (Table 1). The ages are much younger than its depositional ages, which indicates that the samples were completely reset prior before cooling and the maximum paleotemperatures of the Dahongyu and Changzhougou formations are over the ZHe partial annealing zone (~200 °C) (Feng et al., 2021, 2022). The ZHe data recorded the rapid uplift during the Mesozoic. The HeFTy software with the Monte Carlo approach was used to

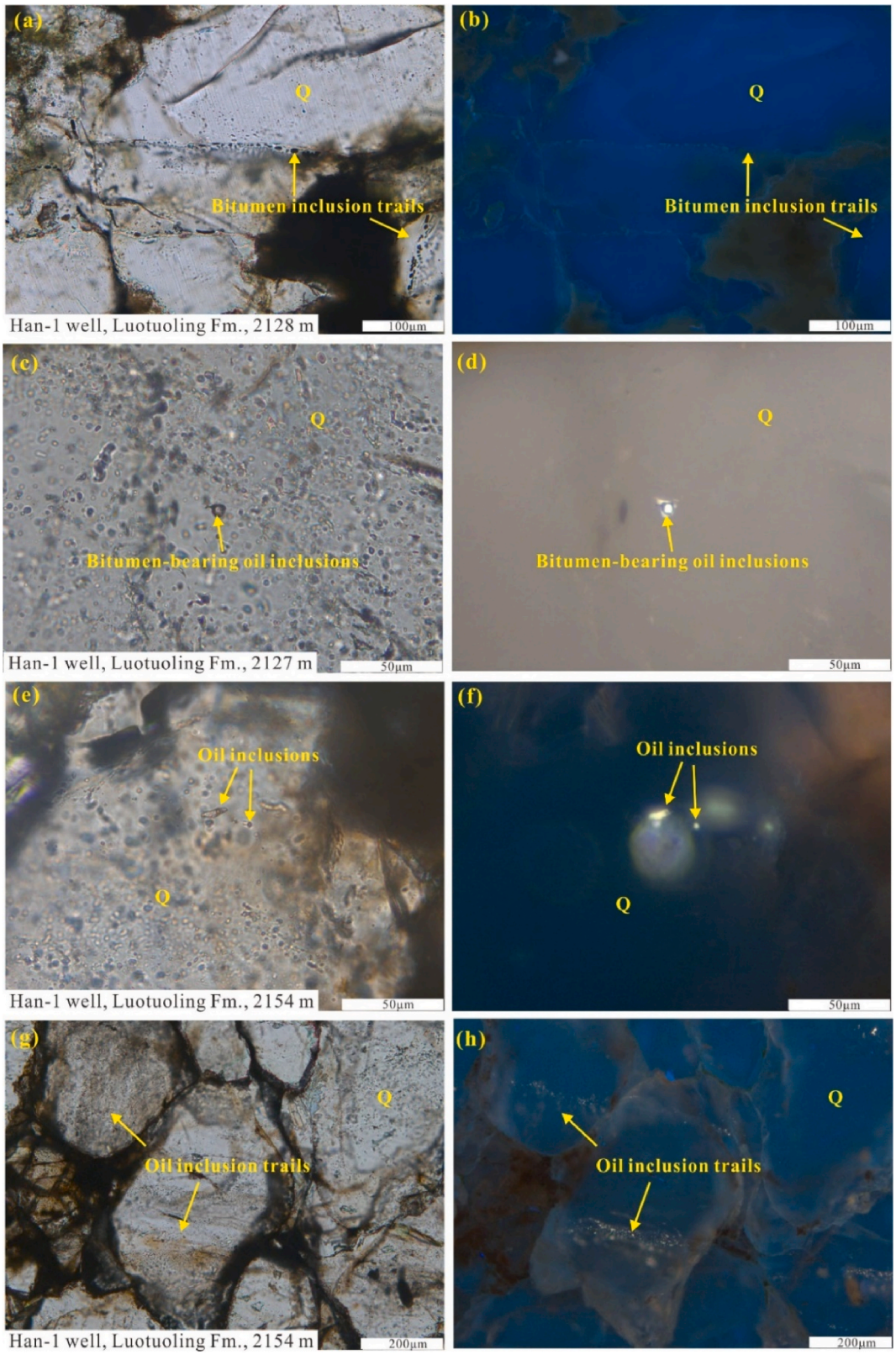

Fig. 4. Photomicrographs of representative oil and bitumen inclusions under transmitted light (left) and UV light (right) observed in the Neoproterozoic Luotuoling Formation in the Liaoxi Depression (Q: quartz). (a–d): trails of bitumen inclusions and bitumen-bearing oil inclusions with white fluorescence along healed micro-fractures at 2125.12–2128.88 m; (e–h): trails of oil inclusions along transgranular micro-fractures with yellowish orange fluorescence at 2153.01–2154.04 m. (For interpretation of the references to color in this figure legend, the reader is referred to the Web version of this article.)

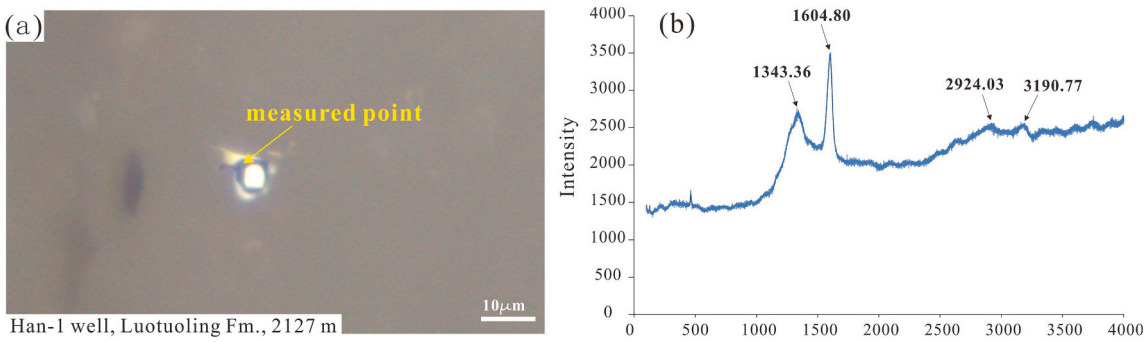

Fig. 5. Bitumen-bearing oil inclusions with the white fluorescence (a) and the Raman spectrum of bitumen (b) in the Neoproterozoic Luotuoling Formation.

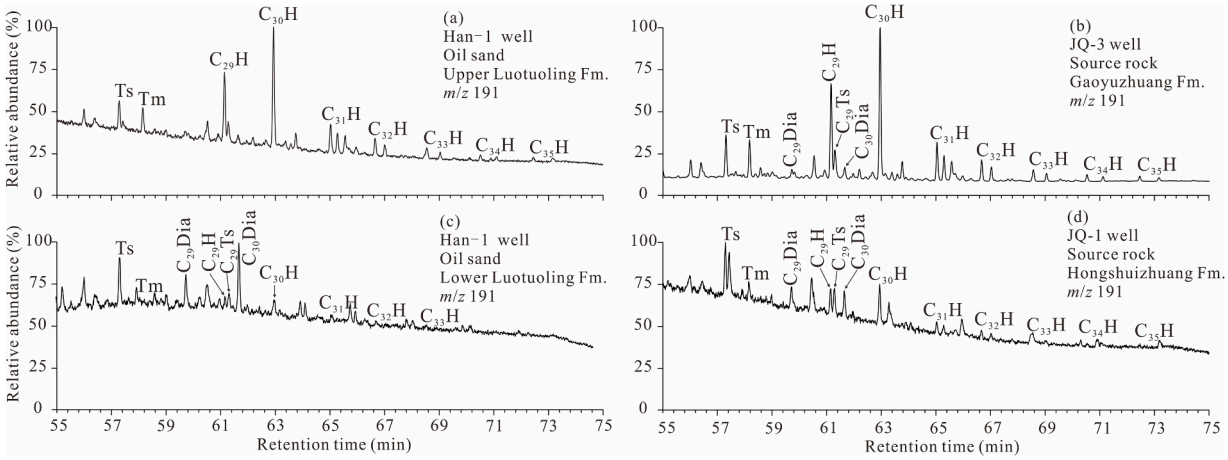

Fig. 6. Representative *m/z* 191 mass chromatograms of the Han-1 well oil sands and source rock extracts. Notes: H = regular hopane; Ts = 18α(H)-neohopane; Dia = 17α(H)-diahopane.

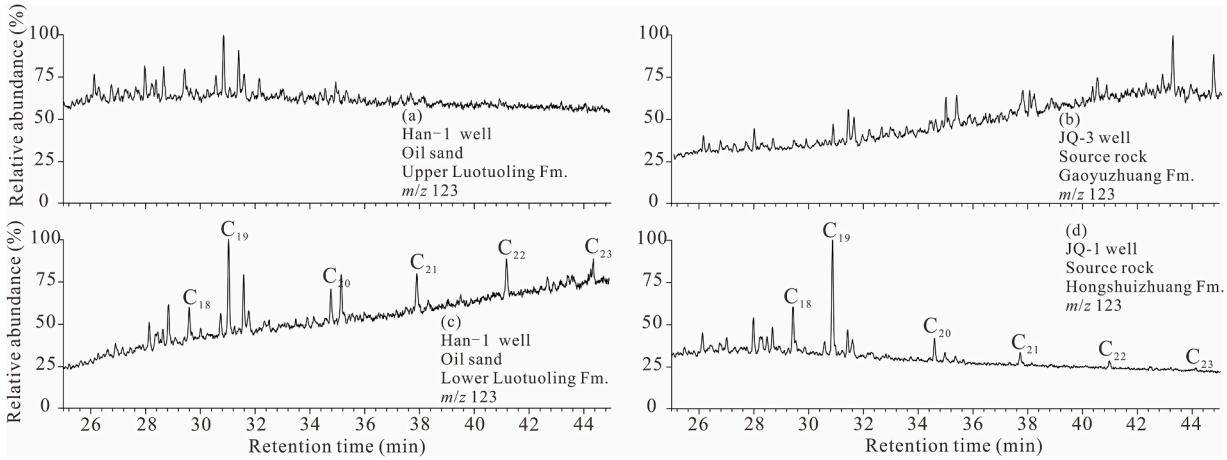

Fig. 7. Representative *m/z* 123 mass chromatograms of the Han-1 well oil sands and source rock extracts. Notes: C_{18}–C_{23}═C_{18}–C_{23} 13α(alkyl)-tricyclic terpanes.

invert the thermal histories (Ketcham, 2005). The zircon radiation damage accumulation and annealing model developed by Guenthner et al. (2013) was selected for the ZHe. In our modelling, the temperature sensitivity ranges of the ZHe were first captured by set the prior temperature range of 20–200 °C in initial modelling process. The present-day surface temperature was set to 20 °C. A total of 1000 thermal paths were developed and we set the range of temperature sensitivities as new constraints. The best-fit time-temperature (t-T) paths indicate the thermal histories of the samples. The modelling results are shown in Fig. 9.

The Dahongyu (LX2) and Changzhougou (LX3) samples experienced generally similar thermal histories. From the Changcheng period to the end of the Jixian period (~1400 Ma), the study area received a rapid deposition (Fig. 8), which making their formation temperature gradually increase (Fig. 9). Then, the study area was in stable tectonic background and experienced a long-terms and slow subsidence before Cambrian period (~541 Ma) (Fig. 8), which corresponds to limited fluctuations of formation temperature (~5 °C), almost at a constant temperature (Fig. 9). Because of the rapid subsidence of the Early Cambrian to Middle Ordovician, the formation temperatures increase

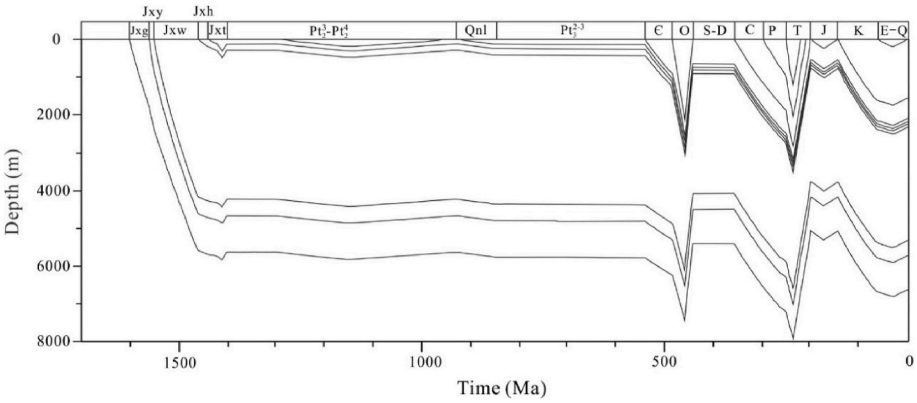

Fig. 8. Reconstructed stratigraphic burial history of the Han-1 well.

Table 1
Zircon (U–Th)/He results of the samples from the Liaoxi Depression, North China Craton.

Sample	Grain radius (μm)	U (ppm)	Th (ppm)	He (nmol/g)	Th/U	Mass (μg)	eU (ppm)	Ft	Corrected age (Ma)	± 1σ (Ma)
LX2-2	39.1	187.94	93.53	124.31	0.51	2.69	209.9	0.718	152.5	8.1
LX2-5	41.6	174.69	100.04	111.15	0.59	2.98	198.2	0.734	141.4	7.5
LX2-8	41.4	213.72	173.05	156.02	0.84	2.96	254.4	0.731	155.0	8.2
LX3-5	38.8	99.96	30.40	86.51	0.33	2.38	171.2	0.72	130.1	6.9
LX3-7	37.4	165.49	37.40	177.01	0.29	2.21	317.3	0.71	145.5	7.7
LX3-8	33.7	159.37	50.20	86.37	0.23	1.80	174.3	0.681	134.9	7.6

Notes: Ft is the α-ejection correction (Farley et al., 1996); eU is effective uranium concentration, which is equal to U+0.235 × Th ppm (Flowers et al., 2009).

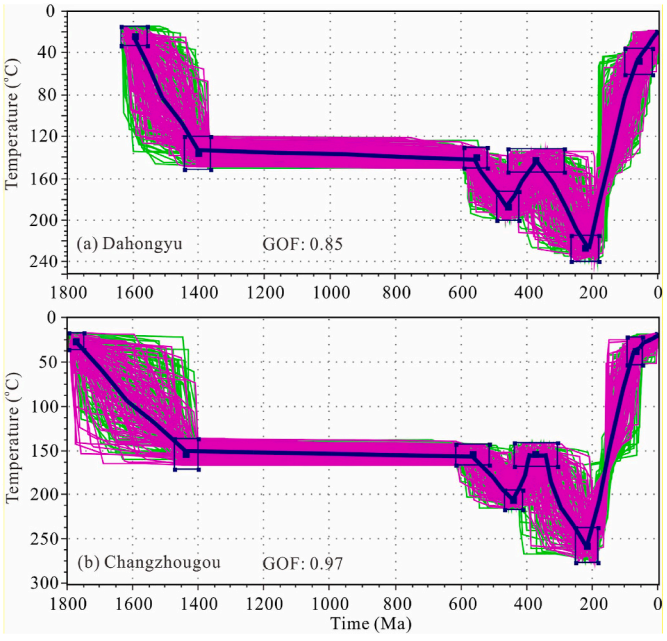

Fig. 9. Thermal histories of the Dahongyu (LX2) and Changzhougou (LX3) samples. Magenta lines represent "good" paths (GOF >0.5), green lines represent "acceptable" paths (GOF >0.05), and blue line is the best modeled thermal history. (For interpretation of the references to color in this figure legend, the reader is referred to the Web version of this article.)

again with the deep burial of more than 7000 m (Fig. 8). In addition, the study area experienced two cooling stages, which are mainly caused by the rapid uplift of the Caledonian and Indosinian orogeny (Fig. 9). Most importantly, because of the strata deep burial and high paleo-heat flow caused by the destruction of the North China Craton (Qiu et al., 2014; Zhang et al., 2014), the paleo-temperatures of these two samples reached their maximum in the Late Triassic (~230 Ma) (Fig. 9).

4.3.3. Heat flow

In this study, the bitumen reflectance (R_B) of nine samples of the Cretaceous, Cambrian and Proterozoic collected from the Han-1 well were measured. According to the conversion relationship between vitrinite reflectance (R_V) and R_B (Jacob, 1989), the equivalent R_V of these R_B were calculated. The equivalent R_V data shows a positive correlation with depth, and the abnormally high values of the equivalent R_V (Fig. 10) are probably caused by magma intrusion. As we all know, the heat flow history can be effectively simulated using R_V data as constraints by the Easy %R_o model in BasinMod 1D software (Sweeney and

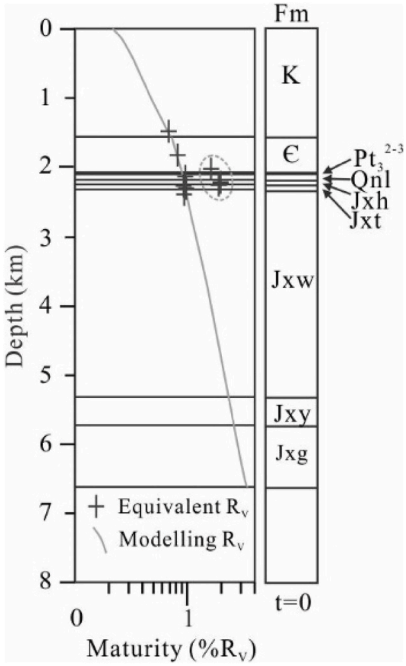

Fig. 10. Calibration of vitrinite reflectance with depth in the Han-1 well.

Burnham, 1990). Firstly, based on the reconstruction of the burial history (Fig. 8), we set the constraint conditions including the equivalent R_V data, present surface temperature (20 °C) and the present-day heat flow values (48 mW/m^2). Secondly, we repeatedly modified the heat flow evolution paths until the modelling R_V path are consistent with the calculated equivalent R_V data (Sinninghe Damste et al., 1995; Mastalerz et al., 2018). Here we found that the calculated maturity profile is consistent overall with that measured (Fig. 10). Therefore, the modeled stratigraphic burial and thermal histories are reliable and practical (Li et al., 2010).

Finally, the paleo-heat flow modelling result indicates that the heat flow of the Han-1 well in the Liaoxi Depression during the Proterozoic has remained relatively stable within the value range of 44–50 mW/m^2. Since Cambrian, it began to increase gradually and reached a maximum value of 70 mW/m^2 in the Triassic period, which was primarily caused by the Indosinian Movement, and then rapidly decreasing to current value of 48 mW/m^2 (Fig. 11).

4.3.4. Oil generation history

Organic matter in source rock gradually transforms into oil and gas as the burial depth and/or temperature increases (Welte and Tissot, 1984). This process is an irreversible reaction controlled by chemical kinetics (Welte and Tissot, 1984; Schenk et al., 1997; Helgeson et al., 2009). In the petroleum generation modelling, the basic geochemical indicators of source rocks include total organic carbon, hydrogen index and kerogen type were in Table 2. Based on the burial history, heat flow history, and geochemical characteristics of source rocks, the maturation evolution histories of Mesoproterozoic Gaoyuzhuang and Hongshuizhuang source rocks were modeled.

The Gaoyuzhuang Formation black argillaceous dolomite and the Hongshuizhuang Formation black shale are potential source rocks in the study area. Their maturity histories were simulated for the Han-1 well in the Liaoxi Depression (Fig. 12a). The modelling result reveals that the oil generation of the Gaoyuzhuang source rocks began approximately 1530 Ma with a temperature of 100 °C at a depth of 3400 m, which is consistent with the threshold depth of oil generation in the Jibei Depression (Wang et al., 2016). The maturity of the Gaoyuzhuang source rocks reached 0.7% R_o equivalent at 1500 Ma, and peak oil generation began at 1460 Ma with a temperature of 120 °C. After 1300 Ma, oil generation of the Gaoyuzhuang source rocks gradually ended with only a small amount of hydrocarbons having been generated (Fig. 12b).

The Hongshuizhuang source rock had two phases of oil generation. During the first phase, due to the deep burial process during the Early to Middle Ordovician, the Hongshuizhuang Formation reached the threshold temperature (100 °C) of oil generation at approximately 460 Ma. Subsequently, the uplift and erosion caused by the Caledonian orogeny (Late Ordovician) suspended oil generation of the Hongshuizhuang Formation source rock (Fig. 12b). This first phase was a short-term maturation process with very limited oil generation, not reaching the threshold of hydrocarbon expulsion from the Hongshuizhuang source rock. The second phase of the Hongshuizhuang source rock occurred at approximately 275–230 Ma, which is significant with respect to oil accumulation in the Liaoxi Depression. The oil generation of the Hongshuizhuang source rock was renewed at approximately 275 Ma with a temperature of 110 °C. Massive oil generation began at 250 Ma, and reached peak oil generation at 240 Ma. As the Indosinian orogeny caused rapid uplift during the late Triassic (Zhang et al., 2014), the Hongshuizhuang Formation source rock gradually stopped oil generation after 230 Ma (Fig. 12b). It is worth noting that the maximum temperature experienced by the Hongshuizhuang Formation source rock was not higher than 160 °C, thus it still has resident potential for oil and gas generation (Fig. 12a).

Table 2
Values of geochemical parameters of source rocks for oil generation modelling.

Well	Source rock	Lithology	TOC (wt. %)	HI (mg/g TOC)	Kerogen type
JQ-1	Hongshuizhuang	shale	2.39	250	II_1
JQ-3	Gaoyuzhuang	dolomite	1.45	45	II_1

4.4. Oil accumulation processes

4.4.1. Fluid inclusion microthermometry

In the study, thirty aqueous inclusions coexisting with bitumen inclusions, oil inclusions and bitumen-bearing oil inclusions were measured to understand oil charge time and charge conditions. The homogenization temperature (T_h) of aqueous inclusions is used as the trapping temperature, because the differences between the T_h and trapping temperatures for aqueous inclusions are generally small in most petroliferous basins.

Aqueous inclusions coeval with bitumen and bitumen-bearing oil inclusions (Type I) from the upper Luotuoling Formation in the studied samples have T_h values ranging from 99.5 to 113.4 °C, with a peak temperature range of 100–110 °C (Fig. 13). Type I aqueous inclusions yielded $T_{m,\ ice}$ from −13.7 to −19.1 °C (from 17.52 to 21.75 wt% NaCl. eqv) (Fig. 14). Whereas coeval aqueous inclusions with yellowish orange fluorescence oil inclusions (Type II) from the Lower Luotuoling Formation were homogenized to a liquid phase at temperatures of 138.2–159.4 °C with a peak temperature range of 140–160 °C (Fig. 13). Type II aqueous fluid inclusions yield $T_{m,\ ice}$ between −4.2 and −9.2 °C

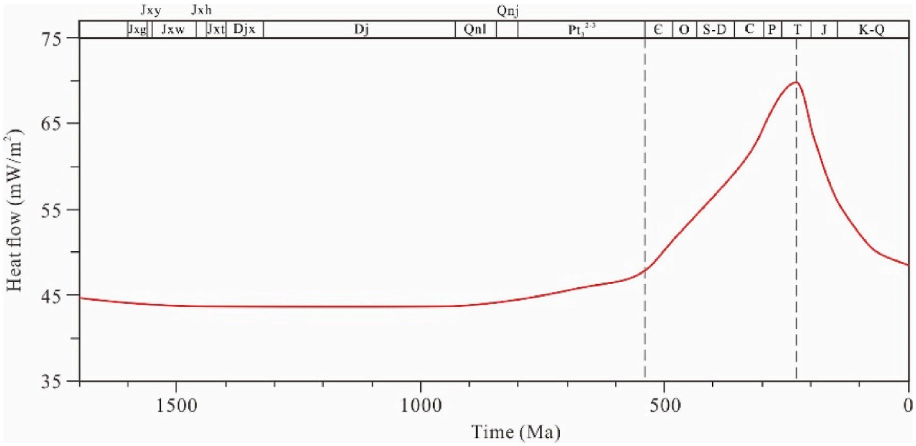

Fig. 11. Heat flow evolution of Han-1 well in the Liaoxi Depression.

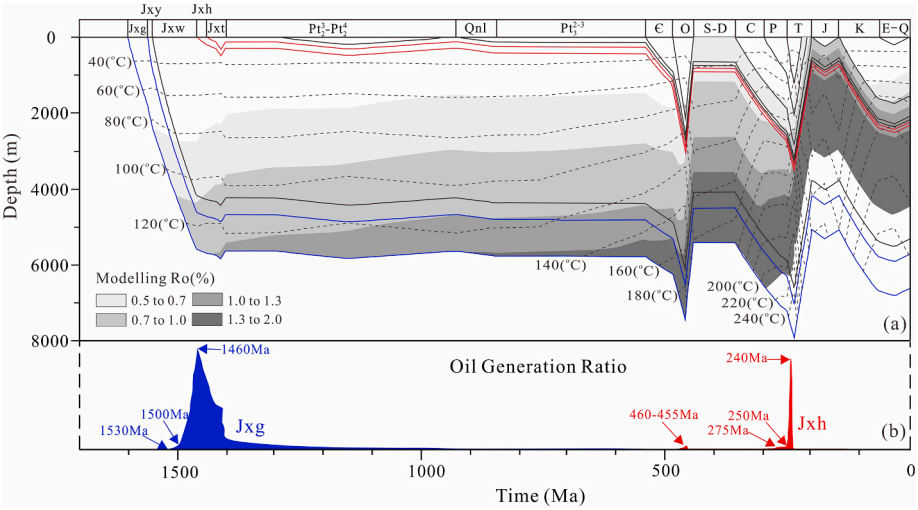

Fig. 12. (a) Reconstructed burial history and thermal maturity history of the Gaoyuzhuang and Hongshuizhuang formations for the Han-1 well in the Liaoxi Depression; (b) Oil generation ratios of the Gaoyuzhuang and Hongshuizhuang formations.

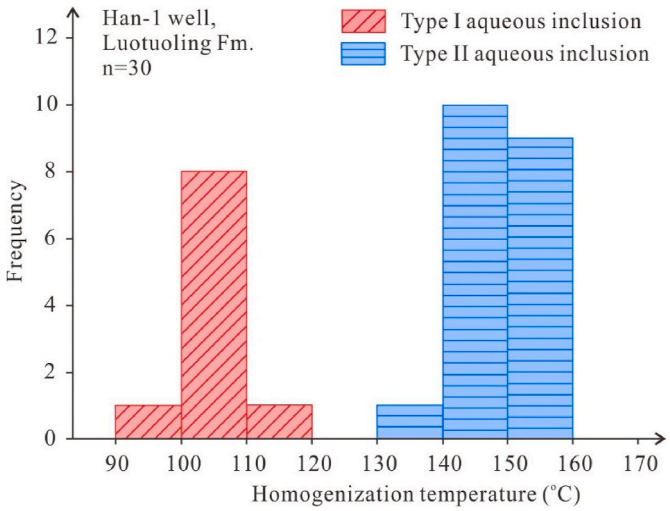

Fig. 13. Histograms showing the distribution of the homogenization temperature of aqueous fluid inclusions in the Neoproterozoic Luotuoling Formation.

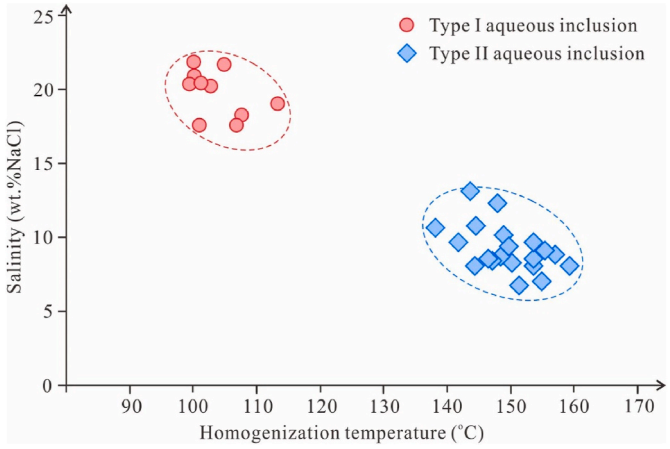

Fig. 14. Homogenization temperatures versus salinities of fluid inclusions in the Neoproterozoic Luotuoling Formation.

(from 6.74 to 13.07 wt% NaCl. eqv) (Fig. 14). The difference of salinities between the two groups of fluid inclusions may be caused by different physicochemical conditions and compositions of the two diagenetic fluids, which indicates the filling of two stages of diagenetic fluid. The histograms of homogenization temperature in Fig. 13 and the scatter plot of salinity in Fig. 14 show that the Neoproterozoic Luotuoling Formation reservoir have two oil charge episodes (Figs. 13 and 14).

4.4.2. *Episodes and time of oil charge*

Combined thermal and reconstructed stratigraphic burial histories with homogenization temperatures, the oil charge time of the Neoproterozoic Luotuoling Formation oil reservoirs was determined. In the study, the T_h values of analyzed fluid inclusions were mainly distributed in the ranges of 100–110 °C and 140–160 °C, and the Luotuoling Formation reached these two temperatures at approximately 465–455 Ma and 240–230 Ma, respectively (Fig. 15). The result illustrates that two episodes of oil charge can be established for the Luotuoling Formation in the Liaoxi Depression, which took place in the Middle to Late Ordovician (465–455 Ma) and the Middle to Late Triassic (240–230 Ma), respectively (Fig. 15). The fluid inclusions trapped in the first oil charge episode are characterized by low temperatures (100–110 °C) and high salinities (17.52–21.75 wt% NaCl. eqv) (Fig. 14), which are coeval with the bitumen inclusions (Fig. 4a and b) and bitumen-bearing oil inclusions (Fig. 4c and d). The aqueous fluid inclusions trapped in the second oil charge episode are coeval with abundant oil inclusions with yellowish orange fluorescence (Fig. 4e–h), and have the characteristic of relatively higher temperature (140–160 °C) than that of the first episode, but lower salinities (6.74–13.07 wt% NaCl. eqv) than the first episode (Fig. 14).

4.4.3. *Oil accumulation stages*

4.4.3.1. Phase I: 1500–1300 Ma. Based on the basin model results of the Han-1 well, the Gaoyuzhuang Formation began to generate hydrocarbon at 1530 Ma, and entered into peak oil generation and expulsion stage at 1500 Ma. These oils were probably accumulated in the Wumishan Formation dolomite, Tieling Formation limestone and Xiamaling sandstones (Fig. 16) (Wang and Han, 2011; Sun and Wang, 2016), with the faults, fractures and microcracks acting as the main migration conduits.

4.4.3.2. Phase II: 465–455 Ma. Based on the analyses of fluid inclusions and burial history, there was an oil charge event in the upper Luotuoling

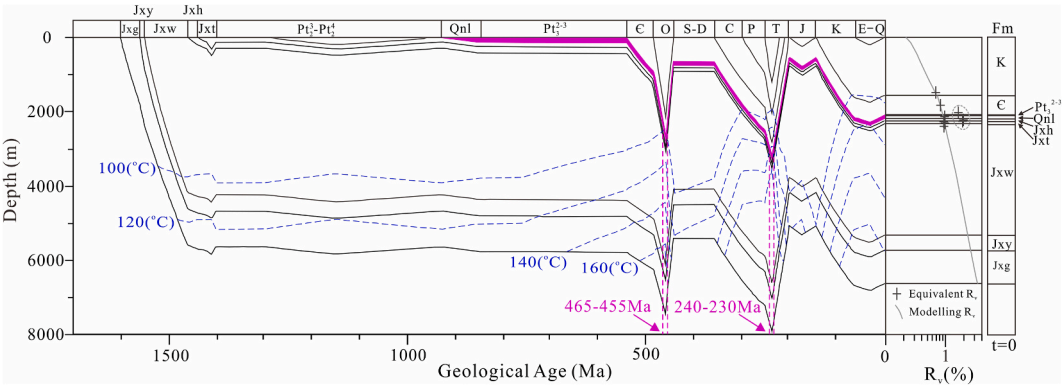

Fig. 15. Episodes and time of oil charge of the Luotuoling Formation oil reservoir in the Han-1 well in the Liaoxi Depression.

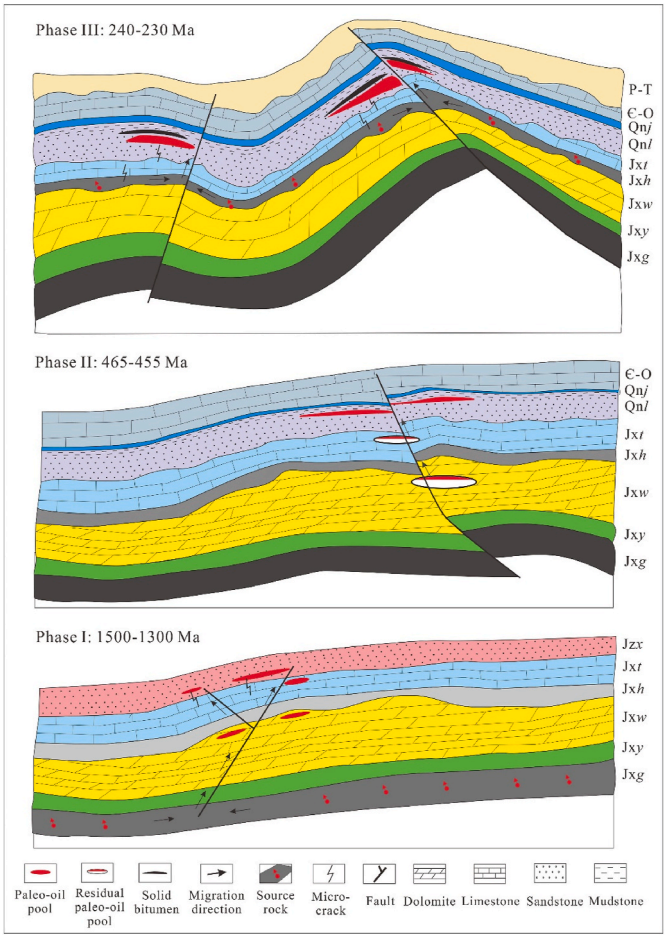

Fig. 16. Schematic model of the Proterozoic paleo-oil reservoir evolution in the Liaoxi Depression.

Formation sandstone reservoirs during the Middle to Late Ordovician (~465–455 Ma). The oils in the upper Luotuoling Formation reservoirs were originated from the Gaoyuzhuang Formation source rock on the basis of oil to source rock correlation analysis. However, the oil generation history of the Gaoyuzhuang source rock show that it became overmature during the Ordovician without oil generation capacity (Fig. 12). The oil generation history of the Hongshuizhuang source rock shows that it had reached the threshold of oil generation at 460 Ma (Fig. 12), but the oil generation process was rapidly suspended due to the uplift during the Late Ordovician, and had not reached the threshold for hydrocarbon expulsion (Fig. 12) (Liu et al., 2011). Therefore, the oils in the upper Luotuoling Formation reservoir cannot be generated directly from the Gaoyuzhuang Formation and Hongshuizhuang source rocks, but probably originated from destroyed paleo-oil reservoirs. In conclusion, the upper Luotuoling Formation oil reservoirs are probably secondary oil reservoirs, which were formed by readjustment and redistribution of paleo-oil reservoirs during the Middle to Late Ordovician (~465–455 Ma) (Fig. 16).

4.4.3.3. Phase III: 240–230 Ma. During the Late Permian to Middle Triassic, there was an oil charge event in the lower Luotuoling Formation sandstone reservoirs (~240–230 Ma) (Fig. 16). Within this period, the Hongshuizhuang Formation source rock entered peak oil generation and expulsion based on the modeled oil generation history (Fig. 12). Furthermore, the oils in the lower Luotuoling Formation were determined to be derived from the Hongshuizhuang Formation source rock based on oil to source rock correlation analysis. The upper Luotuoling Formation oil reservoirs generated from the Gaoyuzhuang Formation source rock had undergone thermal degradation, biodegradation or/and oxidation, most of the oils had been turned into solid bitumen and then blocked the pore spaces (Fig. 3a and b). According to the burial history and paleo-temperature of the Luotuoling Formation (Fig. 12), the solid bitumen may be formed by both biodegradation and thermal degradation. After the oil accumulation in Late Ordovician, the burial depth of the Luotuoling Formation was less than 1000 m during Silurian to Devonian periods, which is a possible reason for the destruction of paleo-oil accumulations in the upper Luotuoling Formation. Then, during Late Permian to Middle Triassic, the paleo-temperature was in the range of 120–160 °C (Waples, 2000), which may lead to the occurrence of thermal cracking of the crude oils accumulated in the Upper Luotuoling Formation. Therefore, the oils generated from the Hongshuizhuang Formation source rock can only be charged into the lower Luotuoling Formation sandstone and formed oil reservoirs.

5. Conclusions

Based on the analyses of biomarker and isotope compositions, the upper and lower Luotuoling Formation sandstone oil reservoirs present different oil sources, which were derived from the Mesoproterozoic Gaoyuzhuang and Hongshuizhuang source rocks, respectively.

Two episodes of oil charge were determined in the Luotuoling Formation reservoirs of the Han-1 well. The first episode, resulting in bitumen emplacement and bitumen-bearing oil inclusions took place at approximately 465–455 Ma in the upper Luotuoling Formation sandstone reservoir (2125.12–2128.88 m). Combined with oil generation history, burial history and oil to source rock correlation analyses, it is likely that the upper Luotuoling Formation sandstone is a secondary oil reservoir formed by remigration from Wumishan or Tieling paleo-oil accumulations which were likely generated from the Gaoyuzhuang Formation source rock.

The second episode recorded by the yellowish orange fluorescent oil inclusions occurred in the lower Luotuoling Formation sandstone reservoir (2153.01–2154.04 m) during approximately 240–230 Ma. These oils were directly generated from the Hongshuizhuang Formation source rocks.

Credit author statement

Hong Xiao: Writing – original draft; Writing – review & editing, Tieguan Wang: Supervision; Conceptualization, Meijun Li: Supervision; Conceptualization, Dongxia Chen: Methodology, Jian Chang: Resources, Daofu Song: Data curation, Chengyu Yang: Methodology. Yingjie Hu: Funding acquisition, Sajjad Ali: Writing – review & editing

Declaration of competing interest

The authors declare that they have no known competing financial interests or personal relationships that could have appeared to influence the work reported in this paper.

Acknowledgements

The authors would like to thank the executive editor and two reviewers for their constructive comments and suggestions which significantly improved the quality of the manuscripts. This research was supported by the Liaohe Oilfield Company, CNPC, China (Oil Accumulation Mechanism of Meso-Neoproterozoic Oil Reservoir in the Liaoxi Depression, NE China) (No. LHYT-KTKFYJY-2018-JS-9798).

References

Bodnar, R.J., 1993. Revised equation and table for determining the freezing point depression of H2O-Nacl solutions. Geochem. Cosmochim. Acta 57, 683–684.
Burruss, R., Cercone, K., Harris, P., 1985. Time of hydrocarbon migration, evidence from fluid inclusions in calcite cements, tectonics and burial history. Soc. Econ. Paleontol. Mineral. Spec. Publ. 36, 277–289.
Craig, J., Thurow, J., Thusu, B., Whitham, A., Abutarruma, Y., 2009. Global neoproterozoic petroleum systems: the emerging potential in north africa. Geol. Soc. Londn. Spec. Publ. 326, 1–25.
Crick, I.H., Boreham, C., Cook, A.C., Powell, T.G., 1988. Petroleum geology and geochemistry of Middle Proterozoic McArthur Basin, northern Australia II: assessment of source rock potential. AAPG (Am. Assoc. Pet. Geol.) Bull. 72, 1495–1514.
Dai, Z., Cai, X., Huang, L., Rao, H., 2014. Numerical simulation of burial history and source rocks maturity evolution history in the Liaoning area. Shandong Chem. Indust. 43, 92–93 (in Chinese with English abstract).
Dutta, S., Bhattacharya, S., Raju, S.V., 2013. Biomarker signatures from neoproterozoic–early cambrian oil, western India. Org. Geochem. 56, 68–80.
Evans, N.J., Byrne, J.P., Keegan, J.T., Dotter, L.E., 2005. Determination of uranium and thorium in zircon, apatite, and fluorite: application to laser (U-Th)/He thermochronology. J. Anal. Chem. 60, 1159–1165.
Farley, K.A., Wolf, R.A., Silver, L.T., 1996. The effects of long alpha-stopping distances on (U-Th)/He ages. Geochimica et Cosmochimica Acta 60, 4223–4229.
Farrimond, P., Telnæs, N., 1996. Three series of rearranged hopanes in Toarcian sediments (northern Italy). Org. Geochem. 25, 165–177.
Feng, Q., Qiu, N., Borjigin, T., Wu, H., Zhang, J., Shen, B., Wang, J., 2022. Tectonic evolution revealed by thermo-kinematic and its effect on shale gas preservation. Energy 240, 122781.
Feng, Q., Qiu, N., Fu, X., Li, W., Xu, Q., Li, X., Wang, J., 2021. Permian geothermal units in the Sichuan Basin: implications for the thermal effect of the Emeishan mantle plume. Mar. Petrol. Geol. 132, 105226.
Flowers, R.M., Ketcham, R.A., Shuster, D.L., Farley, K.A., 2009. Apatite (U–Th)/He thermochronometry using a radiation damage accumulation and annealing model. Geochimica et Cosmochimica Acta 73, 2347–2365.
Fowler, M.G., Douglas, A.G., 1987. Saturated hydrocarbon biomarkers in oils of late precambrian age from eastern Siberia. Org. Geochem. 11, 201–213.
Gao, L., Chuanheng, Z., Liu, P., Feng, T., Biao, S., Xiaozhong, D., 2009. Reclassification of the Meso and neoproterozoic chronostratigraphy of north China by SHRIMP zircon ages. Acta Geol. Sin-Engl. 83, 1074–1084.
Gao, L., Ding, X., Cao, Q., Zhang, C., 2010. New geological time scale of late precambrian in China and geochronology. Chin. Geol. 37, 1014–1020 (in Chinese with English abstract).
Gao, L., Ding, X., Pang, W., Zhang, C., 2011. New geologic time scale of Meso- and Neoproterozoic of China and geochronologic constraint by SHRIMP zircon U-Pb dating. J. Stratigr. 35, 1–7 (in Chinese with English abstract).
Gao, L., Zhang, C., Yin, C., Shi, X., Wang, Z., Liu, Y., Liu, P., Tang, F., Song, B., 2008b. SHRIMP zircon ages: Basis for refining the chronostratigraphic classification of the Meso- and Neoproterozoic strata in North China old land. Acta Geoscientica Sinica 29, 366–376.
Gautheron, C., Tassan-Got, L., Barbarand, J., Pagel, M., 2009. Effect of alpha-damage annealing on apatite (U–Th)/He thermochronology. Chem. Geol. 266, 157–170.
George, S.C., Ruble, T.E., Dutkiewicz, A., Eadington, P.J., 2001. Assessing the maturity of oil trapped in fluid inclusions using molecular geochemistry data and visually-determined fluorescence colours. Appl. Geochem. 16, 451–473.
Goldstein, R.H., 2001. Fluid inclusions in sedimentary and diagenetic systems. Lithos 55, 159–193.
Goldstein, R.H., Reynolds, T.J., 1994. Systematics of Fluid Inclusions in Diagenetic Minerals [M]. SEPM Society for Sedimentary Geology.
Grantham, P.J., Lijmbach, G.W.M., Posthuma, J., 1990. Geochemistry of crude oils in Oman. Geol. Soc. Londn. Special Public. 50, 317–328.
Grantham, P.J., Lijmbach, G.W.M., Posthuma, J., Clarke, M.W.H., Willink, R.J., 1987. Origin of crude oils in Oman. J. Petrol. Geol. 11, 61–80.
Guenthner, W.R., Reiners, P.W., Ketcham, R.A., Nasdala, L., Giester, G., 2013. Helium diffusion in natural zircon: radiation damage, anisotropy, and the interpretation of zircon (U-Th)/He thermochronology. Am. J. Sci. 313 (3), 145–198.
Guo, H., Du, Y., Kah, L.C., Huang, J., Hu, C., Huang, H., Yu, W., 2013. Isotopic composition of organic and inorganic carbon from the Mesoproterozoic Jixian Group, North China: implications for biological and oceanic evolution. Precambrian Res. 224, 169–183.
Hao, S., Feng, S., 1982. Paleotemperature Evolution of Sinian Sub-erathem in North China and Origin of Primary Oil and Gas Pools. Journal of the University of Petroleum China, pp. 1–17 (in Chinese with English abstract).
Helgeson, H.C., Richard, L., Mckenzie, W.F., Norton, D.L., Schmitt, A., 2009. A chemical and thermodynamic model of oil generation in hydrocarbon source rocks. Geochem. Cosmochim. Acta 73, 594–695.
Jackson, M.J., Powell, T.G., Summons, R.E., Sweet, I.P., 1986. Hydrocarbon shows and petroleum source rocks in sediments as old as 1.7 × 10 9 years. Nature 322, 727–729.
Jacob, H., 1989. Classification, structure, genesis and practical importance of natural solid oil bitumen ("migrabitumen"). Int. J. Coal Geol. 11, 65–79.
Ketcham, R.A., 2005. Forward and inverse modeling of low-temperature thermochronometry data. Rev. Mineral. Geochem. 58, 275–314.
Killops, S.D., Howell, V.J., 1991. Complex series of pentacyclic triterpanes in a lacustrine sourced oil from Korea Bay Basin. Chem. Geol. 91, 65–79.
Kuznetsov, V.G., 1997. Riohean hydrocarbon reservoirs of the yurubchen-tokhom zone, lena-tunguska Province, NE Russia. J. Petrol. Geol. 20, 459–474.
Li, C., Peng, P.a., Sheng, G., Fu, J., Yan, Y., 2001. A biomaekers study of Paleo- to Neo-proterozoic (1.8~0.85 Ga) sediments from the Jixian strata section , North China. Earth Sci. Front. 8, 463-462 (in Chinese with English abstract).
Li, C., Peng, P.a., Sheng, G., Fu, J., Yan, Y., 2003. A molecular and isotopic geochemical study of Meso- to Neoproterozoic (1.73–0.85 Ga) sediments from the Jixian section, Yanshan Basin, North China. Precambrian Res. 125, 337–356.
Li, H., Lu, S., Li, H., Sun, L., Xiang, Z., gENG, J., Zhou, H., 2009. Zircon and beddeleyite U-Pb precision dating of basic rock sills intruding Xiamaling Formation, North China. Geol. Bull. China 28, 1396–1404 (in Chinese with English abstract).
Li, H., Su, W., Zhou, H., Xiang, Z., Tian, H., Yang, L., Warren, D.H., Frank, R.E., 2014. The first precise age constraints on the Jixian System of the Meso- to Neoproterozoic Standard Section of China: SHRIMP zircon U-Pb dating of bentonites from the Wumishan and Tieling formations in the Jixian Section, North China Craton. Acta Petrologica Sinica 30, 2999–3012.
Li, M., Wang, T., Chen, J., He, F., Yun, L., Akbar, S., Zhang, W., 2010. Paleo-heat flow evolution of the tabei uplift in tarim basin, northwest China. J. Asian Earth Sci. 37, 52–66.
Liu, B., Fang, J., 1989. On petroleum source and maturation characteristics of the organic matter of Cambrian and Middle-Upper Proterozoic in Kuancheng region of Northern Heibei Province. Petrol. Geol. Exp. 11, 16–32 (in Chinese with English abstract).
Liu, Y., Zhong, N., Song, T., Tian, Y., Han, H., He, X., 2011. Hydrocarbon kinetics of mesoproterozoic Hongshuizhuang formation in open system of yanshan area. J. Oil Gas Technol. (J. Jianghan Petroleum Inst.) 33, 17–21 (in Chinese with English abstract).
Lu, S., Yang, C., Li, H., Chen, Z., 2002. North China continent and Columbia supercontinent. Earth Sci. Front. 9, 225–233 (in Chinese with English abstract).
Luo, G., Hallmann, C., Xie, S., Ruan, X., Summons, R.E., 2015. Comparative microbial diversity and redox environments of black shale and stromatolite facies in the Mesoproterozoic Xiamaling Formation. Geochem. Cosmochim. Acta 151, 150–167.
Luo, Q., George, S.C., Xu, Y., Zhong, N., 2016. Organic geochemical characteristics of the Mesoproterozoic Hongshuizhuang Formation from northern China: implications for thermal maturity and biological sources. Org. Geochem. 99, 23–37.
Magoon, L.B., Dow, W.G., 1994. The Petroleum System.
Mastalerz, M., Drobniak, A., Stankiewicz, A.B., 2018. Origin, properties, and implications of solid bitumen in source-rock reservoirs: a review. Int. J. Coal Geol. 195, 14–36.
McLimans, R.K., 1987. The application of fluid inclusions to migration of oil and diagenesis in petroleum reservoirs. Appl. Geochem. 2, 585–603.
Meng, Q.-R., Wei, H.-H., Qu, Y.-Q., Ma, S.-X., 2011. Stratigraphic and sedimentary records of the rift to drift evolution of the northern North China craton at the Paleo- to Mesoproterozoic transition. Gondwana Res. 20, 205–218.
Moldowan, J.M., Fago, F.J., Carlson, R.M.K., Young, D.C., van Duyne, G., Clardy, J., Schoell, M., Pillinger, C.T., Watt, D.S., 1991. Rearranged hopanes in sediments and petroleum. Geochem. Cosmochim. Acta 55, 3333–3353.
Murray, G.E., Kaczor, M.J., Mcarthur, R.E., 1980. Indigenous precambrian petroleum revisted. AAPG (Am. Assoc. Pet. Geol.) Bull. 64, 1681–1700.

Ni, Z., Wang, T., Li, M., Fang, R., Li, Q., Tao, X., Cao, W., 2016. An examination of the fluid inclusions of the well RP3-1 at the Halahatang Sag in Tarim Basin, northwest China: implications for hydrocarbon charging time and fluid evolution. J. Petrol. Sci. Eng. 146, 326–339.
Niu, S., Xin, H., 2013. Stratigraphycal correlation of the Qingbaikou system and establish of the Jinzhou system. Geol. Surv. Res. 36, 1–9 (in Chinese with English abstract).
Ourisson, G., Rohmer, M., Poralla, K., 1987. Prokaryotic hopanoids and other polyterpenoid sterol surrogates. Annu. Rev. Microbiol. 41, 301–333.
Peng, P.a., Sheng, G., Fu, J., Yan, Y., 1998. Biological markers in 1.7 billion year old rock from the Tuanshanzi Formation, Jixian strata section, North China. Org. Geochem. 29, 1321–1329.
Peng, Y., Bao, H., Yuan, X., 2009. New morphological observations for paleoproterozoic acritarchs from the chuanlinggou formation, north China. Precambrian Res. 168, 223–232.
Peters, K.E., Clark, M.E., Das Gupta, U., McCaffrey, M.A., Lee, C.Y., 1995. Recognition of an infracambrian source rock based on biomarkers in the baghewala-1 oil, India1. AAPG (Am. Assoc. Pet. Geol.) Bull. 79, 1481–1493.
Philp, R.P., Gilbert, T.D., 1986. Biomarker distributions in Australian oils predominantly derived from terrigenous source material. Org. Geochem. 10, 73–84.
Qiao, X., Gao, L., Zhang, C., 2007. New idea of the Meso- and Neoproterozoic chronostratigraphic chart and tectonic environment in Sino-Korean Plate. Geol. Bull. China 26, 503–509 (in Chinese with English abstract).
Qiu, N., Zuo, Y., Chang, J., Li, W., 2014. Geothermal evidence of Mesozoic and Cenozoic lithospheric thinning in the eastern North China craton: constraints from the thermal history of the Jiyang sub-basin, Bohai Bay Basin. Gondwana Res. 26, 1079–1092.
Qu, Y., Zhu, S., Whitehouse, M., Engdahl, A., McLoughlin, N., 2018. Carbonaceous biosignatures of the earliest putative macroscopic multicellular eukaryotes from 1630 Ma Tuanshanzi Formation, north China. Precambrian Res. 304, 99–109.
Schenk, J., Horsfield, B., Krooss, B., Schaefer, G., Schwochau, K., 1997. Petroleum and Basin Evolution, pp. 231–269.
Sinninghe Damste, J.S., Kenig, F., Koopmans, M.P., Koster, J., Schouten, S., Hayes, J.M., de Leeuw, J.W., 1995. Evidence for gammacerane as an indicator of water column stratification. Geochem. Cosmochim. Acta 59, 1895–1900.
Stasiuk, L.D., Snowdon, L.R., 1997. Fluorescence micro-spectrometry of synthetic and natural hydrocarbon fluid inclusions: crude oil chemistry, density and application to petroleum migration. Appl. Geochem. 12, 229–241.
Sun, S., Wang, T., 2016. Meso-Neoproterozoic Geology and Oil and Gas Resources in East China [M]. Science Press, Beijing, pp. 403–430, 2016.
Sweeney, J., Burnham, A., 1990. Evaluation of a simple model of vitrinite reflectance based on chemical kinetics. AAPG Bulletin 10 (10), 1559–1570.
Tang, D., Shi, X., Ma, J., Jiang, G., Zhou, X., Shi, Q., 2017. Formation of shallow-water glaucony in weakly oxygenated Precambrian ocean: an example from the Mesoproterozoic Tieling Formation in North China. Precambrian Res. 294, 214–229.
Tang, D., Shi, X., Wang, X., Jiang, G., 2016. Extremely low oxygen concentration in mid-Proterozoic shallow seawaters. Precambrian Res. 276, 145–157.
Terken, J.M.J., Frewin, N.L., 2000. The dhahaban petroleum system of Oman. AAPG (Am. Assoc. Pet. Geol.) Bull. 84, 523–544.
Vermeesch, P., 2010. HelioPlot, and the treatment of overdispersed (U–Th–Sm)/He data. Chem. Geol. 271, 108–111.
Volk, H., George, S.C., 2019. Using petroleum inclusions to trace petroleum systems – a review. Org. Geochem. 129, 99–123.
Volk, H., George, S.C., Dutkiewicz, A., Ridley, J., 2005. Characterisation of fluid inclusion oil in a Mid-Proterozoic sandstone and dolerite (Roper Superbasin, Australia). Chem. Geol. 223, 109–135.
Wang, G., Li, S., Li, X., Zhao, W., Zhao, S., Suo, Y., Liu, X., Somerville, I., Liu, Y., Zhou, J., Wang, Z., 2019. Destruction effect on Meso-Neoproterozoic oil-gas traps derived from Meso-Cenozoic deformation in the North China Craton. Precambrian Res. 333, 105427.
Wang, T., 1980. Primary property of Sinian Suberathem oil seepages and its petroleum geological significance. Petrol. Explor. Develop. 36–54 (in Chinese with English abstract).
Wang, T., 1989. A novel tricyclic terpane biomarker series. J. Jianghan Petrol. Institut. 11, 117–118 (in Chinese with English abstract).
Wang, T., Han, K., 2011. On Meso-Neoproterozoic primary petroleum resources. Acta Petrol. Sin. 31, 1–7 (in Chinese with English abstract).
Wang, T., Simoneit, B.R., 1988. Approach to the proterozoic Xiamaling formation basal sandstone fossil-oil-reservoir. Oil Gas Geol. 9, 278–287 (in Chinese with English abstract).
Wang, T., Zhong, N., Wang, C., Zhu, Y., Liu, Y., Song, D., 2016. Source beds and oil entrapment-alteration histories of fossil-oil-reservoirs in the Xiamaling formation basal sandstone, Jibei depression. Petrol. Sci. Bull. 1, 24–37 (in Chinese with English abstract).
Wang, T.G., Simoneit, B.R.T., 1995. Tricyclic terpanes in Precambrian bituminous sandstone from the eastern Yanshan region, North China. Chem. Geol. 120, 155–170.
Wang, Z., Wang, X., Shi, X., Tang, D., Stüeken, E., Song, H., 2020. Coupled nitrate and phosphate availability facilitated the expansion of eukaryotic life at circa 1.56 Ga. J. Geophys. Res-Biogeo. 125, e2019JG005487.
Waples, D.W., 1994. Maturity Modeling: Thermal Indicators, Hydrocarbon Generation, and Oil Cracking, vol. 60. AAPG Memoir, pp. 285–306.
Waples, D.W., 2000. The kinetics of in-reservoir oil destruction and gas formation: constraints from experimental and empirical data, and from thermodynamics. Org. Geochem. 31, 553–575.
Welte, D.H., Tissot, B.P., 1984. Petroleum Formation and Occurrence.
Wu, L., Monié, P., Wang, F., Lin, W., Ji, W., Yang, L., 2018. Multi-phase cooling of early cretaceous granites on the jiaodong peninsula, east China: evidence from 40Ar/39Ar and (U-Th)/He thermochronology. J. Asian Earth Sci. 160, 334–347.
Xiao, H., Li, M., Liu, J., Mao, F., Cheng, D., Yang, Z., 2019a. Oil-oil and oil-source rock correlations in the Muglad Basin, Sudan and South Sudan: new insights from molecular markers analyses. Mar. Petrol. Geol. 103, 351–365.
Xiao, H., Li, M., Wang, W., You, B., Leng, J., Han, Q., Ran, Z., Wang, X., Gao, Z., 2021a. Four series of rearranged hopanes in the Mesoproterozoic sediments. Chem. Geol. 573, 120210.
Xiao, H., Li, M., Wang, W., You, B., Liu, X., Yang, Z., Liu, J., Chen, Q., Uwiringiyimana, M., 2019b. Identification, distribution and geochemical significance of four rearranged hopane series in crude oil. Org. Geochem. 138, 103929.
Xiao, H., Wang, T., Li, M., You, B., Zhu, Z., 2021b. Extended series of tricyclic terpanes in the Mesoproterozoic sediments. Org. Geochem. 156, 104245.
Yang, C., Ni, Z., Li, M., Wang, T., Chen, Z., Hong, H., Tian, X., 2018. Pyrobitumen in South China: organic petrology, chemical composition and geological significance. Int. J. Coal Geol. 188, 51–63.
Zhang, N., Tian, Z., Mao, G., Wu, S., Liu, J., Tuo, Q., 2009. Roman spectroscopic characteristivs of bitumen inclusions. Geochimica 38, 174–178 (in Chinese with English abstract).
Zhang, S.H., Zhao, Y., Davis, G.A., et al., 2014. Temporal and spatial variations of Mesozoic magmatism and deformation in the North China Craton: implications for lithospheric thinning and decratonization. Earth Sci. Rev. 131, 49–87.
Zhao, G., Cawood, P., Wilde, S., Sun, M., 2002. Review of global 2.1-1.8 Ga orogens: implications for a pre-Rodinia supercontinent. Earth Sci. Rev. 59, 125–162.
Zhu, S., Chen, H., 1995. Megascopic multicellular organisms from the 1700-million-year-old tuanshanzi Formation in the jixian area, north China. Science 270, 620–622.
Zhu, S., Zhu, M., Knoll, A.H., Yin, Z., Zhao, F., Sun, S., Qu, Y., Shi, M., Liu, H., 2016. Decimetre-scale multicellular eukaryotes from the 1.56-billion-year-old Gaoyuzhuang Formation in north China. Nat. Commun. 7, 11500.
Zhu, Y., Hao, F., Zou, H., Cai, X., Luo, Y., 2007. Jurassic oils in the central Sichuan basin, southwest China: unusual biomarker distribution and possible origin. Org. Geochem. 38, 1884–1896.
Gao, L., Zhang, C., Shi, X., Song, B., Wang, Z., Liu, Y., 2008a. Mesoproterozoic age for Xiamalin Formation in North China Plate indicated by zircon SHRIMP dating. Chinese Sci. Bull. 53, 2617-2623 (in Chinese with English abstract).
Su, W., Li, H., Huff, W.D., Ettensohn, F.R., Zhang, S., Zhou, H., Wan, Y., 2010. SHRIMP U-Pb dating for a K-bentonite bed in the Tieling Formation, North China. Chinese Sci Bull 55, 2197-2206 (in Chinese with English abstract).
Li, H., Su, W., Zhou, H., Geng, J., Xiang, Z., Cui, Y., Liu, W., Lu, S., 2011. The base age of the Changchengian System at the northern North China Craton should be younger than 1670 Ma: Constraints from zircon U-Pb LA-MC-ICPMS dating of a granite-porphyry dike in Miyun County, Beijing. Earth Science Frontiers 18, 108-120 (in Chinese with English abstract).